# CHAPTER 4

# STABILITY AND FAILURE OF SUDDENLY LOADED LAMINATED COMPOSITE PLATE

## 4.1 Introduction

In this chapter, the stability of laminated composite plate subjected to in-plane pulse loads is investigated. The effect of stacking sequence, imperfection, loading duration and pulse loading function is studied. The influence of stacking sequence on the stability of composite square and rectangular plates subjected to in-plane pulse loads are presented. First, the results of convergence and validation studies are presented followed by the results of the present investigation. The results in this chapter are presented in the following subsections:

- Convergence and Validation Studies
    - Convergence and Validation Study of Static Buckling Load
    - Validation of Shock Spectrum
    - Validation of Dynamic Buckling Load of a Plate
    - Validation of Dynamic Buckling Load of an Orthotropic Plate
- Dynamic Buckling Studies
    - Effect of Loading Duration
    - Effect of Loading Function
    - Effect of Imperfection
    - Effect of Rectangular Pulse Load on a Rectangular Plate
    - Effect of Sinusoidal Pulse Load on a Rectangular Plate

## 4.2 Convergence and Validation Studies

The results of the convergence and validation study are presented in this section. The static buckling of a composite plate and the dynamic buckling of an isotropic plate are calculated.

### *4.2.1 Convergence and validation study of static buckling Load*

The convergence and validation studies of a composite plate are presented in this section. The geometry of the plate is shown in Fig. 3.3(a). The buckling boundary conditions are shown in Fig. 3.3(b). Separate pre-buckling boundary conditions (Fig. 4.1) are considered for evaluating the static buckling load of the composite plate. The material properties are presented in Table 3.1 (Narita and Leissa, 1990). The stacking sequence is (θ/-θ/ θ). The geometry of the plate is *b/a*=1 and *b/a*=2 with *b/h*=100; *b*=2m. The non-dimensional static buckling load is calculated using Eqn. 4.1 where '*a'* is the length of the loaded edge and '*h'* is the thickness of the plate. Figure 4.2(a) shows the results of the convergence study of a plate with *b/a*=2 and stacking scheme (θ/-θ/θ); θ=0°. Figure 4.2(b) shows the results of the convergence study of a plate with *b/a*=2 and stacking scheme (θ/-θ/θ); θ=90°. Figure 4.2(c) shows the results of the convergence study of a plate with *b/a*=2 and stacking scheme (θ/-θ/θ/-θ/θ); θ=45°.

Table 4.1 shows the non-dimensional static buckling loads for a plate with *b/a*=2, *b/h*=100 stacking scheme (θ/-θ/θ); θ=0°. Table 4.2 shows the non-dimensional static buckling loads for a plate with *b/a*=2 and stacking scheme (θ/-θ/θ); θ=90°. Table 4.3 shows the non-dimensional static buckling loads for a plate with *b/a*=1 and stacking scheme (θ/-θ/θ); θ=0°. Table 4.4 shows the non-dimensional static buckling loads for a plate with *b/a*=1 and stacking scheme (θ/-θ/ θ/-θ/θ); θ=45°. The results in Table 4.1 - 4.4 are compared with the finite element results from Narita and Leissa (1990) and the corresponding errors are also presented.

$$\bar{P_x} = \frac{P_x\, a^2}{D_0} \tag{4.1}$$

Where, $D_0 = \frac{E_{11} h^3}{12(1-\nu_{21}\nu_{12})}$

and, $\nu_{21} = \left(\frac{E_{22}}{E_{11}}\right)\nu_{12}$

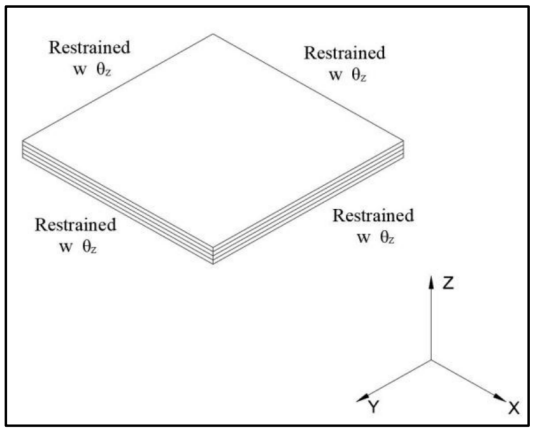


**Fig. 4.1** Pre-buckling boundary conditions for a composite plate

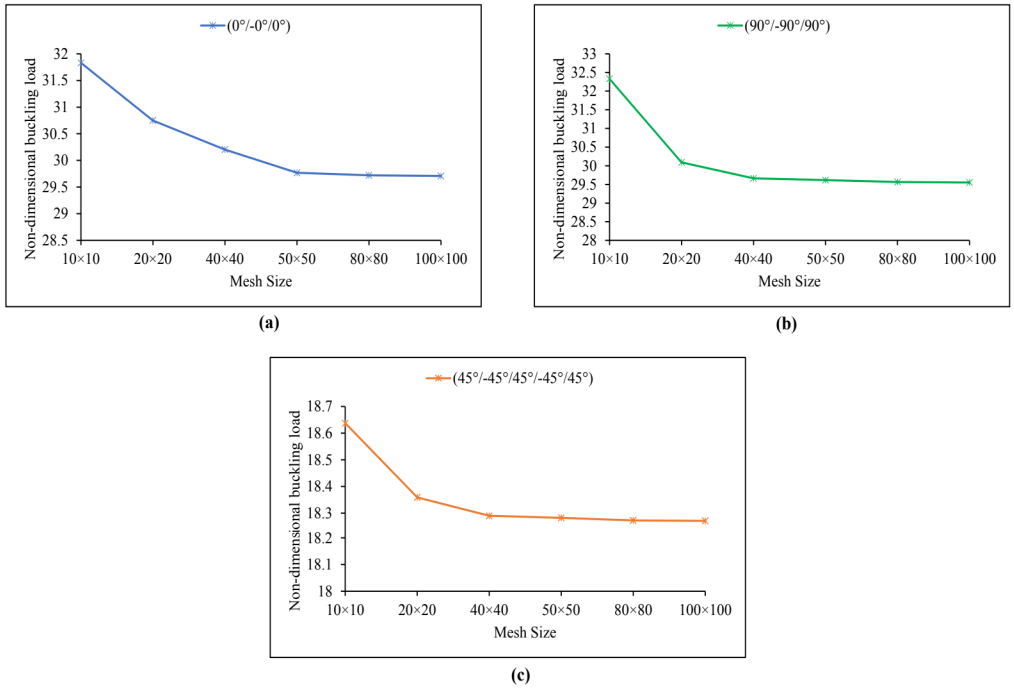


**Fig. 4.2** Convergence study of a plate with *b/h*=100 **(a)** *b/a*=2 and stacking scheme (θ/- θ/ θ); θ=0° **(b)** *b/a*=2 and stacking scheme (θ/- θ/ θ); θ=90° **(c)** *b/a*=1 and stacking scheme (θ/- θ/ θ/- θ/ θ); θ=45°.

**Table 4.1** Non-dimensional static buckling load of a plate with *b/a*=2, *b/h*=100 and stacking scheme (θ/-θ/θ); θ=0°.

| Analysis | Non-dimensional static buckling load | Static buckling load (kN/m) |
|---|---|---|
| Present | 29.77 | 688.71 |
| Narita & Leissa (1990) | 29.74 | - |
| Error (%) | 0.10 | |

**Table 4.2** Non-dimensional static buckling load of a plate with *b/a*=2, *b/h*=100 and stacking scheme (θ/-θ/θ); θ=90°.

| Analysis | Non-dimensional static buckling load | Static buckling load (kN/m) |
|---|---|---|
| Present | 29.62 | 685.17 |
| Narita & Leissa (1990) | 29.74 | - |
| Error (%) | 0.40 | |

**Table 4.3** Non-dimensional static buckling load of a plate with *b/a*=1, *b/h*=100 and stacking scheme (θ/-θ/θ); θ=0°.

| Analysis | Non-dimensional static buckling load | Static buckling load (kN/m) |
|---|---|---|
| Present | 12.89 | 149.21 |
| Narita & Leissa (1990) | 12.91 | - |
| Error (%) | 0.15 | |

**Table 4.4** Non-dimensional static buckling load of a plate with *b/a*=1, *b/h*=100 and stacking scheme (θ/-θ/θ/-θ/θ); θ=45°.

| Analysis | Non-dimensional static buckling load | Static buckling load (kN/m) |
|---|---|---|
| Present | 18.28 | 211.47 |
| Narita & Leissa (1990) | 18.66 | - |
| Error (%) | 2.03 | |

It is observed from Fig. 4.2(a)-4.2(c) that the results converge at a mesh size of 50×50. From Table 4.1-4.4 it is observed that the results of the present study match well with the result from the literature.

### *4.2.2 Validation of shock spectrum*

The shock spectrum of an isotropic plate is validated in this section. A square aluminium plate is subjected to in-plane dynamic pulse load at various loading durations and the maximum transverse deflections of the plate are evaluated. The material properties are $E$ = 70GPa, $v$ = 0.33, $\rho$ = 2950 kg/m$^3$. The geometric properties are $b/a$ = 1, $a$ = 0.5m, $h = 0.005a$. The simply supported boundary condition for the pre-buckling and buckling stage are the same in this case, as shown in Fig. 3.3(b). The initial imperfection is taken as $0.2h$ (= 20% of the thickness of the plate). The imperfection of first buckling mode is incorporated in the plate (Fig. 3.4). The static buckling load is calculated using linear static instability analysis (Eigenvalue), which, in this case is 21648N/m. Then, the first natural period of the plate is calculated ($T_n = 21.36 \times 10^{-3}$ s). Next, non-linear static instability analysis (Riks analysis) is performed to calculate the non-linear static displacement. The equation solved is presented in section 3.3.3 (Post-buckling analysis). The central transverse displacement corresponding to three times static buckling load ($3\times N_{st}$) is calculated with the incorporation of imperfection in the plate ($w_{st}$ = 0.0057m). The plot of $w_{st}$ vs the load is shown in Fig. 4.3(a). For various durations of loading ($T_b$), the transverse displacements ($w_{dyn}$) are calculated using non-linear dynamic analysis (Abaqus/Explicit). The plate is subjected to in-plane sinusoidal pulse load for various durations (Fig. 3.5b). The results of the dynamic analysis are presented along with the finite element results of Azarboni *et al.* (2015) and the numerical results of Petry and Fahlbusch (2000) in Fig. 4.3(b).

It is seen from the Fig.4.3(b) that the peak response for the simply supported isotropic rectangular plate is reached near its first natural period. The results of the current study match with the finite element results of Azarboni *et al.* (2015) and numerical results of Petry and Fahlbusch (2000).

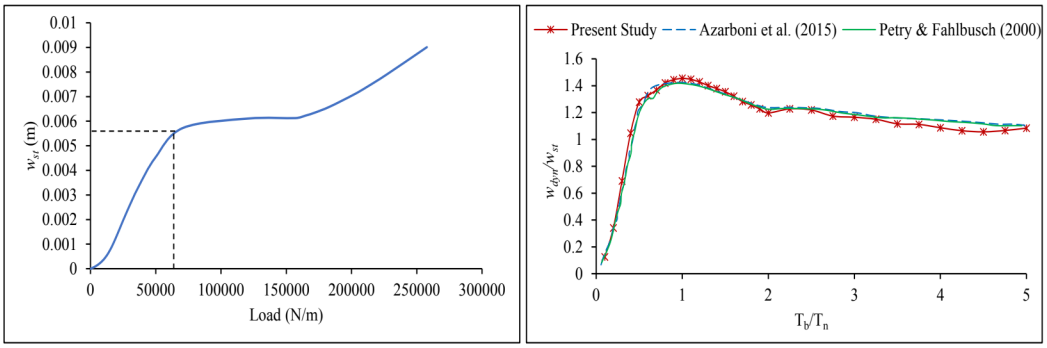


**Fig. 4.3** Plot for a plate with $b/a$=1, $a$=0.5m, $h$= 0.005$a$ and imperfection= 0.2$h$ **(a)** transverse displacement vs in-plane load curve **(b)** Validation study of shock spectrum of the plate subjected to dynamic loading ($N_{dyn}$=3×$N_{st}$)

### *4.2.3 Validation of dynamic buckling load of a plate*

In this section, the dynamic buckling load for an aluminium plate is validated. A square, simply supported plate is subjected to sinusoidal in-plane pulse load (Fig.3.5(b)). The geometric and material properties of the plate are: $b/a$=1, $b/h$=200, imperfection = 5% of plate thickness; $E$=70GPa, $v$=0.3 and $\rho$=2950kg/m$^3$. Imperfection in the plate corresponds to the first buckling mode shape. The duration of loading is the first natural period of the plate. The static buckling load of a perfect plate is 43045N/m calculated using Abaqus/Standard. The simply supported boundary condition for the pre-buckling and buckling stage are the same in this case, as shown in Fig. 3.3(b). The first natural period of the plate=43.176×10$^{-3}$s. For various magnitude of in-plane loads, the maximum transverse displacements are calculated using Abaqus/Explicit. Figure 4.4 shows the plot of non-dimensional load vs non-dimensional displacement for the plate with $b/a$=1, $b/h$=200 and imperfection = 5% subjected to sinusoidal pulse loading for various magnitude of loads. The results of the present study are compared with the analytical-numerical method results of Kubiak (2013), the finite element results of Kowal-Michalska and Mania (2008) and the numerical results of Petry and Fahlbusch (2000).

Petry and Fahlbusch (2000) solved the problem using numerical method using double series solution. Kowal-Michalska and Mania (2008) solved the problem using an eight noded shell element with six degrees of freedom at each node. Kubiak (2013) solved the problem using an analytical-numerical method considering the shear lag and the effect of cross-sectional

distortions. The author compared the results with those presented by Petry and Fahlbusch (2000) and attributed the discrepancies to a more accurate model with higher number of terms in the double series solution adopted by Petry and Fahlbusch (2000). From Fig. 4.4 it is observed that the results of the present study match well with the analytical-numerical study of Kubiak (2013). The variation in the results at the last point ($N_{dyn}/N_{st}$ =4) is 12%. However, the dynamic buckling load with respect to Vol'mir criterion calculated by present study is $1.5N_{st}$, by Petry and Fahlbusch (2000) 1.52 $N_{st}$, by Kowal-Michalska and Mania (2008) is 1.52 $N_{st}$ and by Kubiak (2013) is 1.48 $N_{st}$. Thus, it can be concluded that the dynamic buckling load of the present study matches well with the results from the literature.

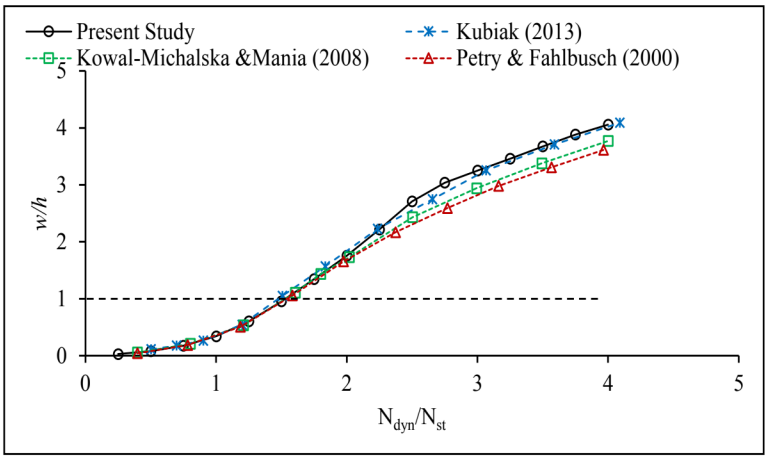


**Fig. 4.4** Validation study of dynamic buckling behaviour of a plate with *b/a*=1, *b/h*=200, imperfection=0.05*h*, subjected to sinusoidal pulse load

### *4.2.4 Validation of dynamic buckling load of an orthotropic plate*

In this section, the dynamic buckling load of an orthotropic plate are evaluated and validated using the results from the literature. The material properties are $E_{11}$=53.781GPa, $E_{22}$=17.927GPa, $v_{12}$=0.25, $v_{21}$=0.083, $G_{12}=G_{23}=G_{31}$=8.964GPa. The geometric properties are *b/a*=1, *b/h*=200 and imperfection =5% of the plate thickness in the form of first buckling mode of the plate. The geometry of the plate is shown in Fig. 3.3(a) and the boundary conditions are shown in Fig.3.3(b). Same boundary conditions are considered for the pre-buckling and buckling stage. The plate is subjected to a rectangular pulse load (Fig. 3.5(a)). The results of the present study are compared with the finite element results of Kowal-Michalska and Mania (2008) in Fig. 4.5.

Kowal-Michalska and Mania (2008) solved the problem using an eight noded shell element with six degrees of freedom at each node. In the present investigation, a four noded shell element with six degrees of freedom is used. In Fig. 4.5 it is seen that the results diverge at higher non-dimensional loads. The variation in results at $N_{dyn}/N_{st}$ =3 is 6.6%. However, the dynamic buckling load with respect to Vol'mir criterion by the present study is $1.12N_{st}$ and by Kowal-Michalska and Mania (2008) is $1.16N_{st}$. Thus, the dynamic buckling load of the present study matches well with the result Kowal-Michalska and Mania (2008).

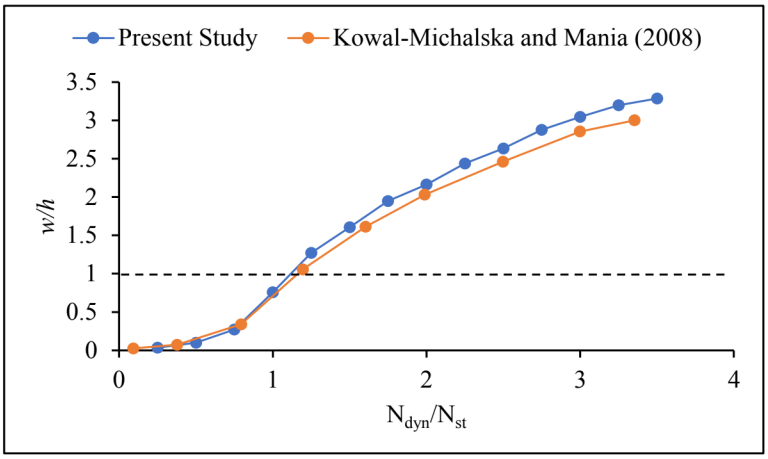


**Fig. 4.5** Validation study of dynamic buckling behaviour of an orthotropic plate with *b/a*=1, *b/h*=200, imperfection=0.05*h*, subjected to rectangular pulse load

It is seen from the convergence and validation studies that the results of the present study match well with the results from the literature. The plate in the present study for evaluating the dynamic buckling load is discretized in a similar way as done in this section. Mesh size of 50×50 is converged and the same mesh size is considered. Further, the boundary conditions taken for the validation studies of shock spectrum and dynamic buckling load i.e., same boundary conditions for pre-buckling and buckling stage is considered to evaluate the static buckling load of the plate and also for cylindrical panels in the next chapters (Chapter 5-7).

## 4.3 Dynamic Buckling Studies

In this section, the results of dynamic buckling studies along with failure studies are presented. The calculation of non-linear dynamic buckling load and the first ply failure load are presented first. The geometry of the plate is shown in Fig. 3.3(a) and the boundary conditions are shown in Fig. 3.3(b). For this, plate with geometry: *b/a*=1, *b/h*=100, imperfection =0.2*h* and the

material properties presented in Table 3.2 are considered. The stacking sequence is (0°/90°/90°/0°). The imperfection 0.2*h* corresponds to 20% of the thickness of the plate in the form of the first buckling mode of the plate (Fig. 3.4). The static buckling load and the first natural period of the plate are calculated and then the plate is subjected to load till its first natural period.

In Fig. 4.6, the plot of non-dimensional time vs non-dimensional displacements are shown. The panel is subjected to rectangular in-plane pulse load till its first natural period and the displacements are observed after the removal of the load. For each magnitude of dynamic load, the panel is subjected to, the maximum transverse displacements are taken into consideration for the plot of non-dimensional load vs non-dimensional displacement (Fig. 4.8). In Fig. 4.8, the deformed shapes of the panel at different magnitude of loads are also presented which are marked in the plot (point 1 corresponds to the maximum displacement for dynamic load=$0.2N_{st}$; point 2 corresponds to the maximum displacement for dynamic load=$0.4N_{st}$ etc.). For instance, in Fig. 4.6, the maximum displacement for the panel when subjected to a dynamic load $N_{dyn}=N_{st}$ (shown in blue colour dash line) is considered and plotted in Fig. 4.8 as point 5. Corresponding to the point 5 marked in the non-dimensional load vs non-dimensional displacement plot, the respective deformed shape of the panel when subjected to rectangular in-plane pulse load having magnitude $N_{dyn}=N_{st}$ is shown. The maximum deformation in the panel is observed at the centre of the panel marked in red colour in Fig.4.8.

Similarly, for various magnitude of dynamic loads, the failure index with respect to different failure theories are considered and the non-dimensional time vs failure index with respect to Tsai-Wu criterion is plotted in Fig. 4.7. In Fig. 4.9, the deformed shapes of the panel at different magnitude of loads are also presented which are marked in the plot (point 1 corresponds to the maximum failure index with respect to Tsai-Wu failure criterion for dynamic load=$0.2N_{st}$; point 2 corresponds to the maximum failure index with respect to Tsai-Wu failure criterion for dynamic load=$0.4N_{st}$ etc.). For instance, in Fig. 4.7, the maximum failure index with respect to Tsai-Wu failure criterion for the panel when subjected to a dynamic load $N_{dyn}=2.2N_{st}$ (shown in green colour dash line) is considered and plotted in Fig. 4.9 as point 9. Corresponding to the point 9 marked in the non-dimensional load vs failure index (Tsai-Wu criterion) plot, the corresponding deformed shape of the panel when subjected to rectangular in-plane pulse load having magnitude $N_{dyn}=2.2N_{st}$ is shown. The maximum deformation in the panel is observed

at the centre of the panel and the region having the maximum failure index is marked in red colour in Fig.4.9.

It is observed from Fig. 4.6 and Fig. 4.7 that the maximum value of the displacement and the failure index occurs during the loading of the plate and not after the removal of the load. Also, the dynamic buckling load of the plate with 20% imperfection is lower than the static buckling load. However, the first ply failure load is much higher than the static buckling load and the dynamic buckling load of the plate. The deformation scale factor in Fig. 4.8 and Fig. 4.9 is 10 and in both cases, the region in red shows the area with maximum displacement and failure index respectively. From Fig. 4.8 and Fig. 4.9 it is observed that the maximum deformation in the plate occurs at the centre of the panel and the location of maximum deformation does not change with change in the magnitude of dynamic load. However, the location of failure changes with the change in the magnitude of the load.

The influence of loading duration, loading function, imperfection and stacking sequence on the dynamic buckling behavior of laminated composite plate is investigated in the following sections. For this investigation, the material properties from Table 3.1 and Table 3.2 are considered. The results of a square plate and rectangular plate are presented in the succeeding sections and the dynamic buckling load and the first ply failure loads are compared with their respective static buckling loads. The static bucking load of the plate with $b/a$=1, $b/h$=100, with $b$=0.1m and stacking sequence is (0°/90°/90°/0°) is 15951N/m and its first natural period is $2.84\times10^{-3}$s. For the case of rectangular plate with $b/a$=2, $b/h$=100 with $b$=0.2m and stacking sequence (θ/-θ/θ), the static buckling load and the first natural period are presented in Table 4.5.

**Table 4.5** Static buckling load and first natural period for the plate with $b/a$=2, $b/h$=100 with $b$=0.2m and stacking sequence (θ°/-θ°/θ°)

| θ | Static buckling load (N/m) | First natural Period (s) |
|---|---|---|
| 0° | 86346 | $2.81\times10^{-3}$ |
| 30° | 226987 | $2.03\times10^{-3}$ |
| 45° | 192154 | $1.67\times10^{-3}$ |
| 60° | 210623 | $1.40\times10^{-3}$ |
| 90° | 127157 | $1.19\times10^{-3}$ |

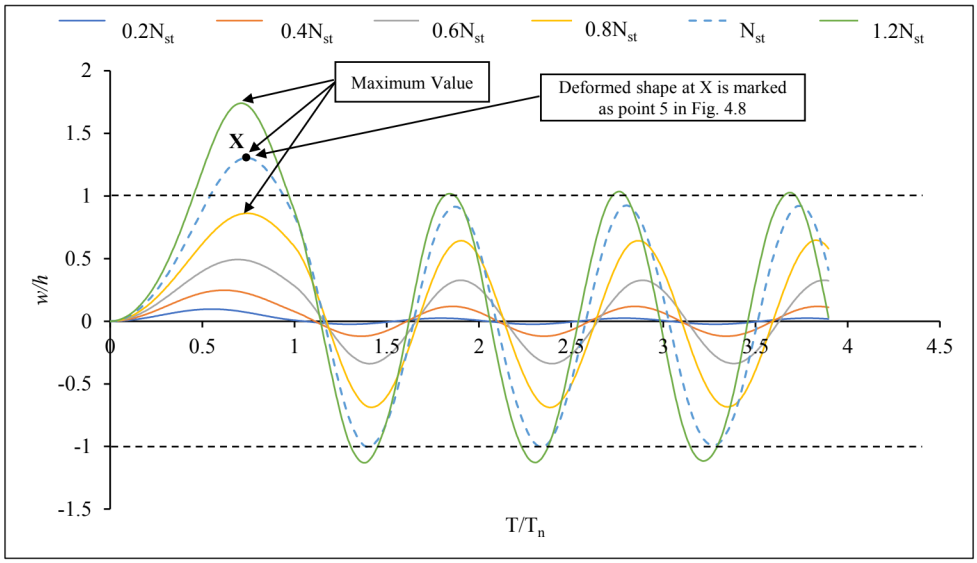


**Fig. 4.6** Non-dimensional Time vs Non-dimentional Displacement for a plate with *b/a*=1, *b/h*=100, imperfection=0.2*h* and stacking sequence (0°/90°/90°/0°), when subjected to rectangular pulse load.

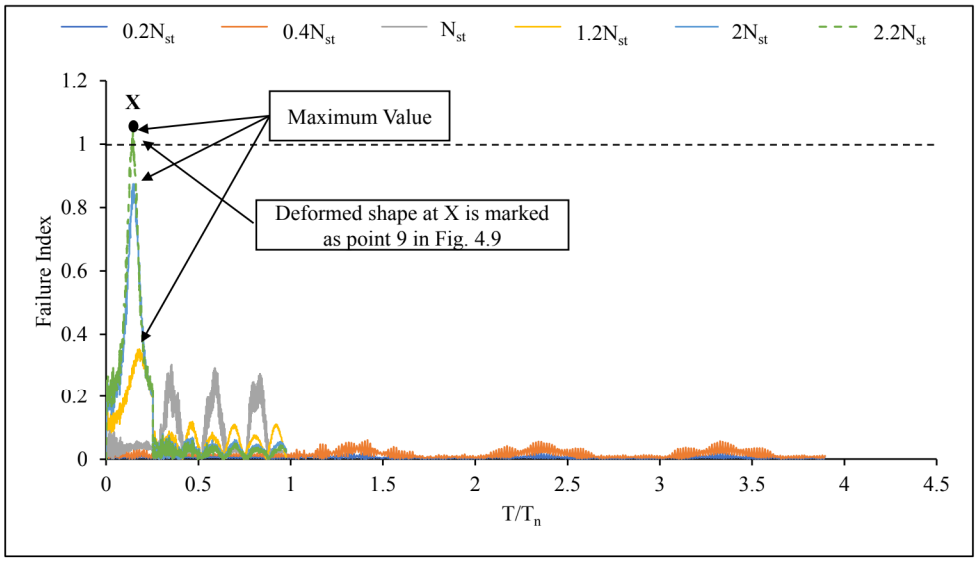


**Fig. 4.7** Non-dimensional Time vs Failure index (Tsai-Wu criterion) for a plate with *b/a*=1, *b/h*=100, imperfection=0.2*h* and stacking sequence (0°/90°/90°/0°), when subjected to rectangular pulse load.

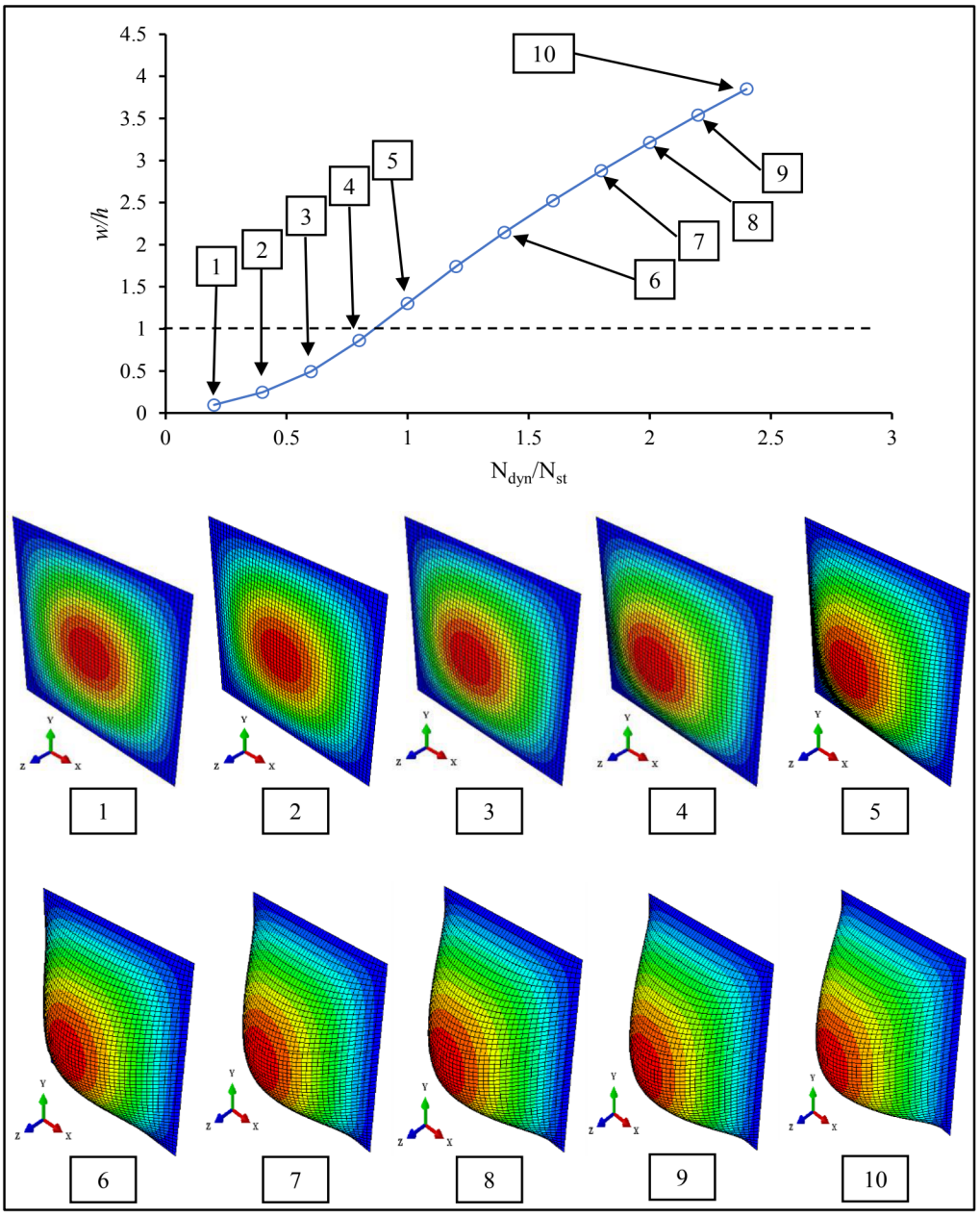


**Fig. 4.8** Non-dimensional Load vs Non-dimensional Displacement along with the of deformation for a plate with *b/a*=1, *b/h*=100, imperfection=0.2*h* and stacking sequence (0°/90°/90°/0°), when subjected to rectangular pulse load. Deformation scale Factor=10.

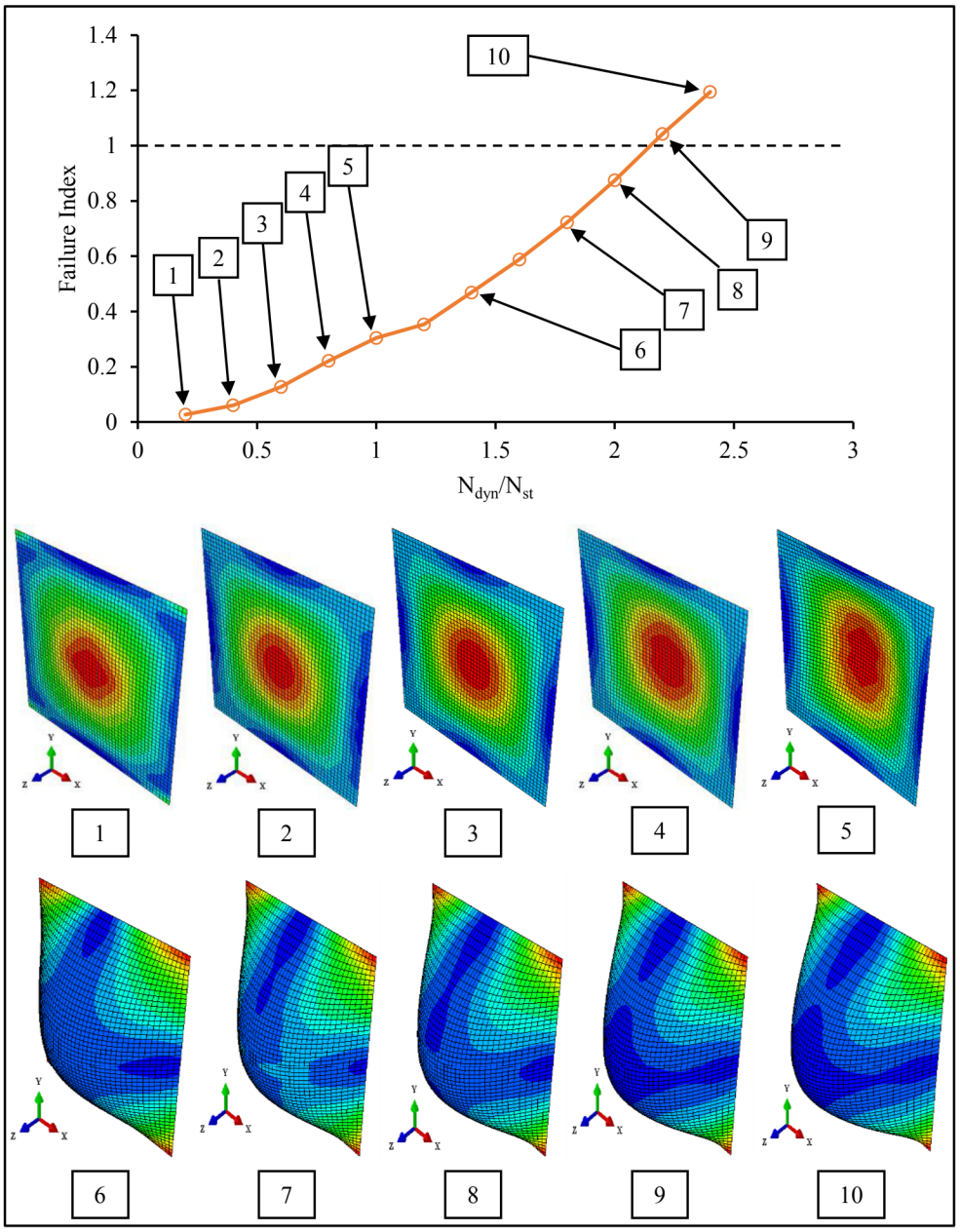


**Fig. 4.9** Non-dimensional Load vs Failure Index (Tsai-Wu criterion) along with the of deformation for a plate with *b/a*=1, *b/h*=100, imperfection=0.2*h* and stacking sequence (0°/90°/90°/0°), when subjected to rectangular pulse load. Deformation scale Factor=10.

### *4.3.1 Effect of loading duration*

In this section, the effect of loading duration on the stability of laminated composite plate subjected to in-plane pulse load is investigated. The stacking sequence is (0°/90°/90°/0°). The geometric properties are: *b/a*=1, *b/h*=100. The material properties are presented in Table 3.2. The procedure for calculating the dynamic buckling load and first ply failure load are described in the previous section. The first natural period ($T_n$) of the plate is calculated and for various ratios of $T_b/T_n$, the responses are observed. The plate is subjected to a rectangular pulse load (Fig. 3.5(a)). Figure 4.10 shows the plot of non-dimensional load vs non-dimensional displacement for laminated composite plate with *b/a*=1, *b/h*=100 imperfection = 0.2*h* for various durations of loading.

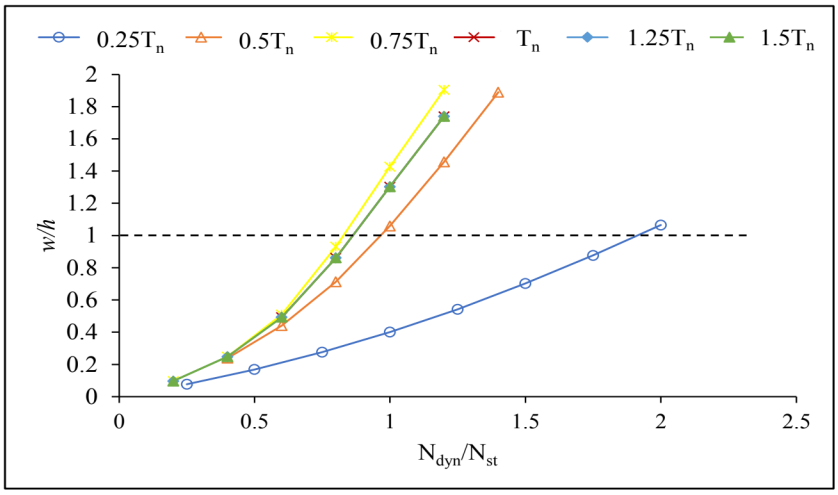


**Fig. 4.10** Non-dimensional Load vs non-dimentional Displacement for composite plate with *b/a*=1, *b/h*=100 imperfection = 20% subjected to rectangular pulse load.

From Fig. 4.10 it is seen that the results converge when the duration of loading is near the first natural period of the plate. Thus, the loading duration near the first natural period of the plate is critical. It is also observed that for a laminated composite plate with 20% of the thickness imperfection in the form of its first buckling mode, the dynamic buckling load is lower than its static buckling load when subjected to a loading duration $T_b/T_n$=0.5 or higher. The panel when subjected to an in-plane dynamic load in the form of rectangular pulse load till $0.75T_n$, its dynamic buckling load is lower than that of the panel when subjected to a load for a duration higher than it. The difference in dynamic buckling load is not much. Thus, in the

present investigation, the plate is subjected to load till its first natural period. The stiffness of the thin laminated composite plate is dependent on the duration of loading. It decreases with the increase in the duration of loading.

### *4.3.2 Effect of loading function*

In this section, the effect of loading function on the stability of a laminated composite plate subjected to in-plane pulse load is investigated. Three types of pulse loading functions are considered: rectangular (Fig. 3.5(a)), sinusoidal (Fig. 3.5(b)) and triangular (Fig. 3.5(c)). The stacking sequence is (0°/90°/90°/0°). Figure 4.11(a) shows the plot of non-dimensional load vs displacement for laminated composite plate with $b/a$=1, $b/h$=100 imperfection = 0.1$h$. Figure 4.11(b) shows the plot of non-dimensional load vs failure index for laminated composite plate with $b/a$=1, $b/h$=100 imperfection = 0.1$h$. The failure criterion considered is Tsai-Wu criterion.

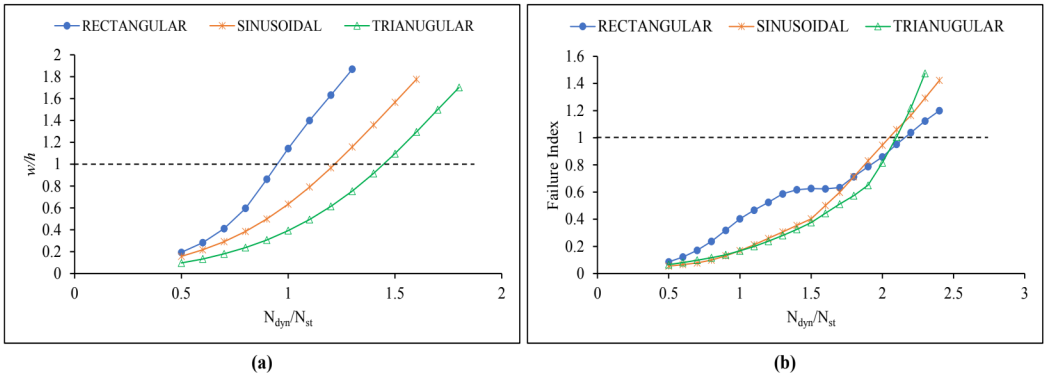


**Fig. 4.11** Plot for laminated composite plate with $b/a$=1 and imperfection =10% for various loading functions **(a)** Non-dimensional Load vs Non-dimentional Displacement **(b)** Non-dimensional Load vs Failure Index (Tsai-Wu criterion)

From Fig. 4.11(a) it is seen that the dynamic buckling load for the plate will be the lowest when subjected to rectangular pulse load. It is observed from Fig. 4.11(b) that the first ply failure load for all the cases is higher than the dynamic buckling load. Thus, the first ply failure occurs after the laminated composite plate buckles due to dynamic pulse loads irrespective of the pulse loading function considered. Furthermore, the first ply failure load for all the cases is at least twice the static buckling load of the plate. It is observed that the stiffness of the plate with imperfection changes with the change in the loading function but, the strength of the plate is not significantly affected. This can be seen in Fig. 4.11 (b) where the fist ply

failure loads of the plate are close to each other. Apart from these observations, a sharp increase in transverse displacement is observed when the plate is subjected to rectangular pulse load (at $N_{dyn}/N_{st}$=0.8), it is not observed in case of sinusoidal or triangular pulse loads. As the area under the plot of time vs load in the case of a rectangular loading function is higher than that of the sinusoidal loading function and triangular loading function, the panel is subjected to a greater energy when subjected to rectangular loading function. In dynamic loading cases, the duration of loading, as well as the magnitude of load is critical. Hence, rectangular loading function gives a higher response compared to the other two loading functions and thus the dynamic buckling load of the plate is lower than the other cases.

### *4.3.3 Effect of imperfection*

The effect of imperfection on dynamic buckling load is studied in this section. For all three types of loading functions, the non-linear dynamic buckling load and first ply failure load are calculated. Four types of imperfection are considered: 5%, 10% and 20% which are percentages of the thickness of the plate and shape is the first buckling mode of the plate (Fig. 3.4). The layup sequence is (0°/90°/90°/0°). Figures 4.12(a), 4.13(a) and 4.14(a) show the plot of non-dimensional load vs displacement for a composite plate with *b/a*=1, *b/h*=100 for rectangular, sinusoidal and triangular loading functions respectively. Figures 4.12(b), 4.13(b) and 4.14(b) show the plot of non-dimensional load vs failure index with respect to Tsai-Wu failure criterion for a composite plate with *b/a*=1, *b/h*=100 for rectangular, sinusoidal and triangular loading functions respectively.

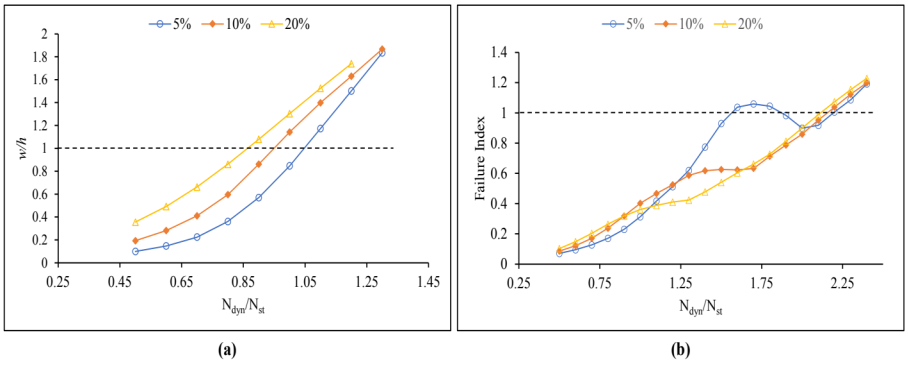


**Fig. 4.12** Plot for laminated composite plate with *b/a*=1 and subjected to rectangular pulse load for various imperfections **(a)** Non-dimensional Load vs non-dimensional Displacement **(b)** Non-dimensional Load vs Failure Index (Tsai-Wu criterion)

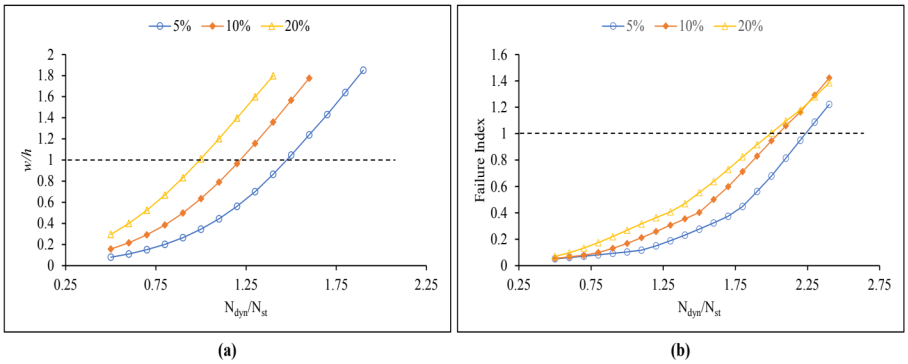


**Fig. 4.13** Plot for laminated composite plate with *b/a*=1 and subjected to sinusoidal pulse load for various imperfections **(a)** Non-dimensional Load vs non-dimensional Displacement **(b)** Non-dimensional Load vs Failure Index (Tsai-Wu criterion)

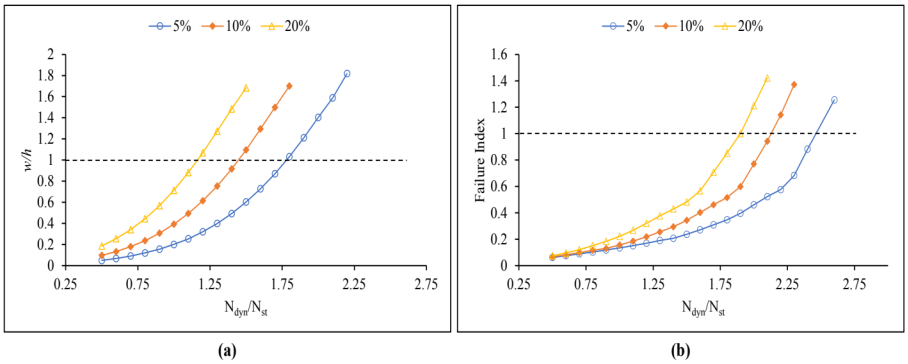


**Fig. 4.14** Plot for laminated composite plate with *b/a*=1 and subjected to triangular pulse load for various imperfections **(a)** Non-dimensional Load vs non-dimensional Displacement **(b)** Non-dimensional Load vs Failure Index (Tsai-Wu criterion)

It is seen from Fig. 4.12 - 4.14 that the dynamic buckling load of the composite plate is lower than the first ply failure load. In the case of a composite plate subjected to rectangular pulse load, the dynamic buckling load is lower than the static buckling load for 10% and 20% imperfection in the plate. For the case of a plate subjected to sinusoidal pulse load, the dynamic buckling load is equal to static buckling load for 20% imperfection in the plate. And in the case where the plate is subjected to triangular in-plane pulse load, the dynamic buckling load of the plate is higher than the static buckling load for all the cases. These results show that the stiffness of a laminated composite plate changes with the imperfection in the plate and also, the pulse loading function considered. In Fig. 4.12(b), the failure index for the plate with 5% imperfection when subjected to rectangular pulse load reaches the value of one and then it

reduces. It is to be mentioned here that the progressive failure in the plate is not calculated. It is also observed in Fig. 4.12(b) that the first ply failure load of the plate with 10% and 20% imperfections are close to each other. In the current investigation, the imperfection shape considered is shown in Fig. 3.4. Due to change in the deformation shape of the plate with change in the imperfection value, the stress distribution in the plate varies. Thus, a variation in the expected result (as seen in Fig. 4.14(b)) is observed.

### *4.3.5 Effect of rectangular pulse load on a rectangular plate*

In this section, the dynamic buckling behavior of a rectangular composite plate when subjected to in-plane rectangular pulse load is evaluated. For the rectangular laminated composite plate considered for the validation study (section 4.2.1), the dynamic buckling loads are evaluated when subjected to in-plane rectangular pulse load till its first natural period. Only the dynamic buckling load is calculated and not the first ply failure load. The material properties are presented in Table 3.1. The geometric properties of the plate considered are $b/a$=2 with $b/h$=100. The stacking sequence of the plate is (θ°/-θ°/θ°), where θ= 0°, 30°, 45°, 60° and 90°. The imperfections taken into consideration are 5%, 10% and 20%. The imperfection value of 5% corresponds to 0.05$h$; i.e., 5% of the thickness of the plate and in the shape of its first buckling mode (Fig. 3.4). For uniformity, the same shape of imperfection is taken for all cases. Figures 4.15(a)- 4.15(e) show the non-linear dynamic buckling for laminated composite plates with θ= 0°, 30°, 45°, 60° and 90° respectively for various imperfections (5%, 10% and 20%).

It is observed from Fig. 4.15(a)- 4.15(e) that the dynamic buckling load of the plate does not change much with a change in imperfection value for the plate with θ= 30°, 45° and 60°. This is because even though the same imperfection shape is given to plate with different stacking sequences when subjected to in-plane pulse loads, each stacking sequence will result in a different deformation shape. These deformed shapes are shown in Fig. 4.16(a)-4.16(e), which are at a critical point of loading. The deformed shapes are for different imperfection values. However, the same trend is observed for the plates with the corresponding stacking sequence. Further, in Fig. 4.15, it is observed that the dynamic buckling load of the plate is higher than its static buckling load even with imperfection as high as 20% of the thickness of the plate when subjected to rectangular pulse load. The rectangular plate with stacking sequence (θ°/-θ°/θ°), exhibits higher stiffness than the plate considered in the previous sections. Thus, the

dynamic performance of a thin laminated composite plate changes with change in geometry and material of the plate.

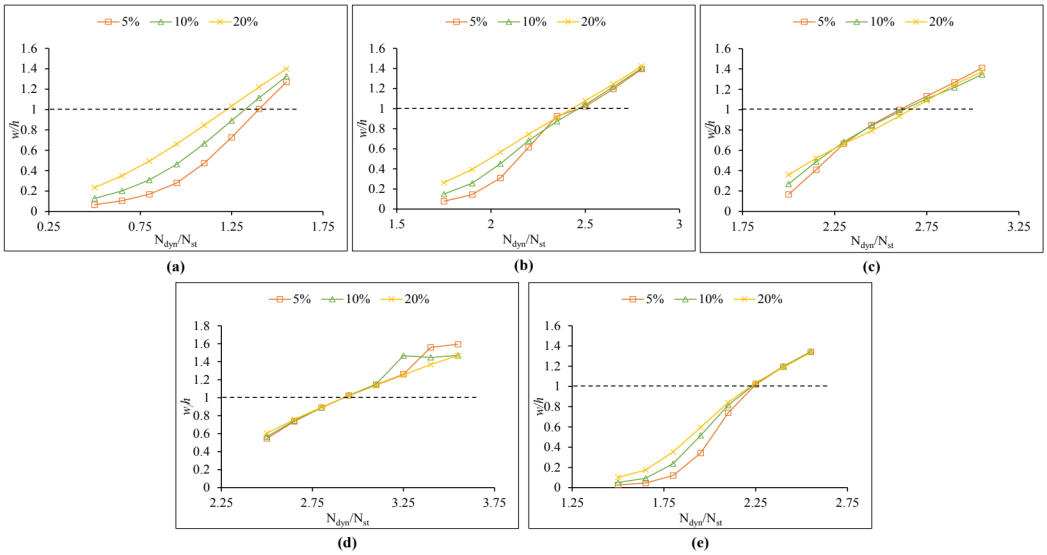


**Fig. 4.15** Non-dimensional Load vs non-dimensional Displacement for laminated composite plate with *b/a* = 2 *b/h*=100 and for various imperfections subjected to rectangular pulse load **(a)** stacking sequence (θ/- θ/ θ), θ=0° **(b)** tacking sequence (θ/- θ/ θ), θ=30° **(c)** tacking sequence (θ/- θ/ θ), θ=45° **(d)** tacking sequence (θ/- θ/ θ), θ=60° **(e)** tacking sequence (θ/- θ/ θ), θ=90°

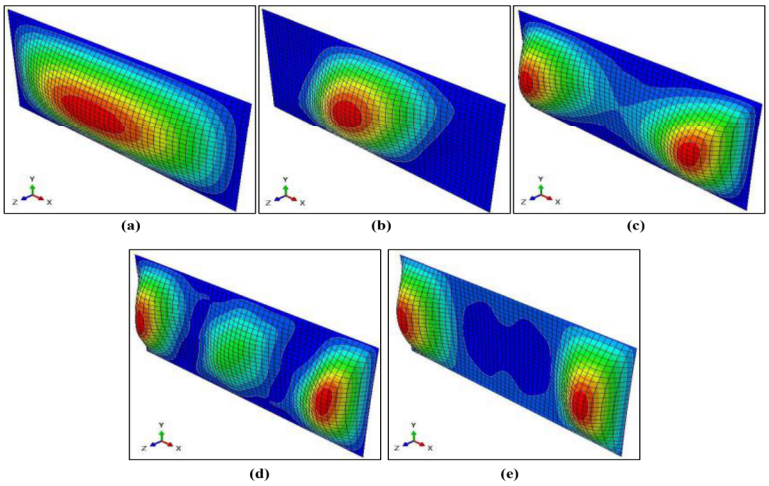


**Fig. 4.16** Deformed shape of the laminated composite plate with *b/a*=2, *b/h*=100, stacking sequence= (θ/- θ/ θ) and subjected to rectangular loading function. imperfection =5%. Deformation scale factor = 10. **(a)**

Imperfection =5% and θ=0° **(b)** Imperfection =10% and θ=30° **(c)** Imperfection =10% and θ=45° **(d)** Imperfection =20% and θ=60° **(e)** Imperfection =5% and θ=90°

### *4.3.6 Effect of sinusoidal pulse load on a rectangular plate*

In this section, the dynamic buckling behavior of a rectangular composite plate when subjected to in-plane sinusoidal pulse load is evaluated. For the rectangular laminated composite plate considered for the validation study (section 5.2.1), the dynamic buckling loads are evaluated when subjected to in-plane sinusoidal pulse load. The material properties are presented in Table 4.1. The geometric properties of the plate are *b/a*=2 and *b/h*=100. The stacking sequence of the plate is (θ/- θ / θ), where θ= 0°, 30°, 45°, 60° and 90°. The imperfections considered are: 5%, 10% and 20%. As reported in the previous section, for uniformity, the same imperfection shape is taken for all cases. Figures 5.31-5.35 show the non-linear dynamic buckling for laminated composite plates with θ= 0°, 30°, 45°, 60° and 90° respectively for various imperfections (5%, 10% and 20%).

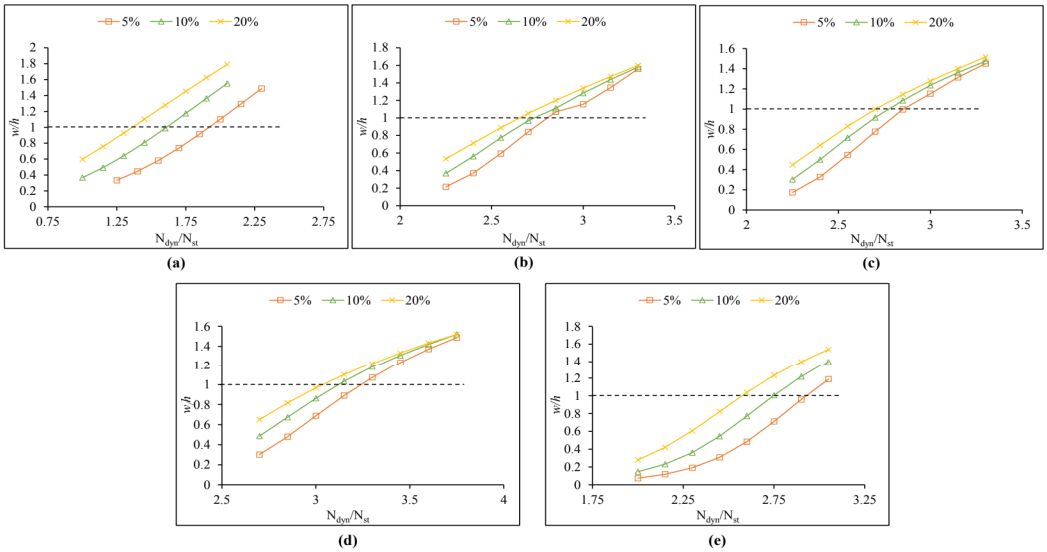


**Fig. 4.17** Non-dimensional Load vs non-dimensional Displacement for laminated composite plate with *b/a* = 2 *b/h*=100 and for various imperfections subjected to sinusoidal pulse load **(a)** stacking sequence (θ/- θ/ θ), θ=0° **(b)** tacking sequence (θ/- θ/ θ), θ=30° **(c)** tacking sequence (θ/- θ/ θ), θ=45° **(d)** tacking sequence (θ/- θ/ θ), θ=60° **(e)** tacking sequence (θ/- θ/ θ), θ=90°

From Fig.5.31-5.35 it is observed that the dynamic buckling load for laminated composite rectangular plates with various stacking sequences even though the imperfection is up to 20%

is higher than their corresponding static buckling load. Considering the plate with stacking sequence (θ/- θ/ θ) with θ=90°, when it is subjected to a rectangular pulse load, for various imperfection values, the dynamic buckling load are very close to each other ($N_{dyn}$=2.25$N_{st}$). However, when the plate is subjected to a sinusoidal in-plane pulse load, for various magnitudes of imperfection values, the dynamic buckling load are far apart ($N_{dyn}$=2.6$N_{st}$-2.9$N_{st}$). This variation is because, in case of a plate subjected to rectangular pulse load, the application and removal of load are sudden. However, in case of a plate subjected to sinusoidal pulse load, the application and removal of the loads are gradual even though the load is acting for a short duration.

## *4.4 Summary*

In this chapter, the non-linear dynamic buckling behaviour of laminated composite plate is studied. The effect of loading duration, pulse loading function and imperfection on the dynamic buckling behaviour of the plate is investigated. The first ply failure of the plate is also calculated to check the precedence of the dynamic buckling load and the first ply failure load. The conclusions drawn from the study are presented in Chapter 8 (Section 8.3).